Science of the Total Environment 933 (2024) 173179

Contents lists available at ScienceDirect

Science of the Total Environment

journal homepage: www.elsevier.com/locate/scitotenv

Captopril's influence on *Danio rerio* embryonic development: Unveiling significant toxic outcomes at environmentally relevant concentrations

Fernando García-Valdespino [1], Gustavo Axel Elizalde-Velázquez [1], Selene Elizabeth Herrera-Vázquez, Leobardo Manuel Gómez-Oliván [*]

Laboratorio de Toxicología Ambiental, Facultad de Química, Universidad Autónoma del Estado de México, Paseo Colón intersección Paseo Tollocan, Colonia Residencial Colón, CP 50120 Toluca, Estado de México, Mexico

HIGHLIGHTS

- Pericardial edema was the main malformation observed in exposed embryos.
- Realistic concentrations of captopril prompted oxidative stress in organisms.
- Apoptosis-, organogenesis-, and ion exchange- related genes were altered.
- Edema formation might be a consequence of pronephros alterations in embryos.

GRAPHICAL ABSTRACT

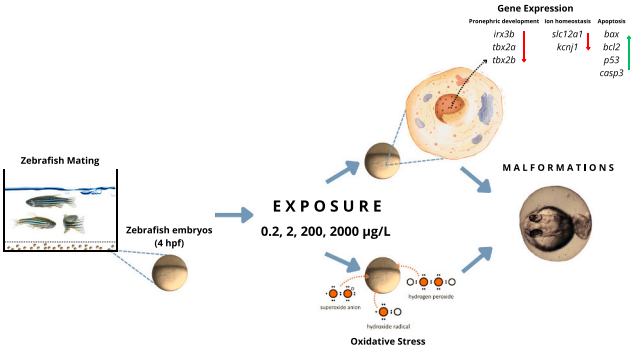

ARTICLE INFO

Editor: Damià Barceló

Keywords:
Antihypertensive drug
Oxidative damage
Embryonic damage
Apoptosis
Zebrafish

ABSTRACT

Anticipating a global increase in cardiovascular diseases, there is an expected surge in the use of angiotensin-converting enzyme inhibitors, notably captopril (CAP). This heightened usage raises significant environmental apprehensions, mainly due to limited knowledge regarding CAP's toxic effects on aquatic species. In response to these concerns, the current study aimed to tackle this knowledge gap by evaluating the potential influence of nominal concentrations of CAP (0.2–2000 µg/L) on the embryonic development of *Danio rerio*. The findings revealed that CAP at all concentrations, even at concentrations considered environmentally significant (0.2 and 2 µg/L), induced various malformations in the embryos, ultimately leading to their mortality. Main malformations included pericardial edema, craniofacial malformation, scoliosis, tail deformation, and yolk sac deformation. In addition, CAP significantly altered the antioxidant activity of superoxide dismutase and catalase across all concentrations. Simultaneously, it elevated lipid peroxidation levels, hydroperoxides, and carbonylic proteins in the embryos, eliciting a substantial oxidative stress response. Likewise, CAP, at all concentrations, exerted significant modulatory effects on the expression of genes associated with apoptosis (*bax, bcl2, p53, and casp3*), organogenesis (*tbx2a, tbx2b, and irx3b*), and ion exchange (*slc12a1 and kcnj1*) in *Danio rerio* embryos. Both augmentation and reduction in the expression levels of these genes characterized this modulation. The Pearson

* Corresponding author at: Laboratorio de Toxicología Ambiental, Facultad de Química, Universidad Autónoma del Estado de México, Paseo Colón intersección Paseo Tollocan, Colonia Residencial Colón, CP 50120 Toluca, Estado de México, Mexico.
E-mail address: lmgomezo@uaemex.mx (L.M. Gómez-Oliván).
[1] These authors contributed equally

https://doi.org/10.1016/j.scitotenv.2024.173179
Received 28 February 2024; Received in revised form 9 May 2024; Accepted 10 May 2024
Available online 13 May 2024

correlation analysis indicated a close association between oxidative damage biomarkers and the expression patterns of all examined genes with the elevated incidence of malformations and mortality in the embryos. In summary, it can be deduced that CAP poses a threat to aquatic species. Nevertheless, further research is imperative to enhance our understanding of the environmental implications of this pharmaceutical compound.

1. Introduction

Captopril (CAP), identified chemically as (2*S*)-1-[(2*S*)-2-methyl-3-sulfanylpropanoyl]pyrrolidine-2-carboxylic acid ($C_9H_{15}NO_3S$), serves as an angiotensin-converting enzyme (ACE) inhibitor and is employed as a thiolated antihypertensive medication (dos Santos et al., 2020). However, its application extends to the management of post-myocardial infarction, heart failure, and the treatment of diabetic nephropathy (Mahmoud and Kümmerer, 2012). Even though the specific global sales figures for CAP may be unclear, it is crucial to emphasize that cardiovascular drugs and lipid-regulating agents are prominent among the most commonly prescribed medications worldwide. For instance, these medications constitute 24.5 % of the top 200 prescribed drugs in the United States (Mc Namara et al., 2019). However, it is noteworthy to mention this prescribing trend is not exclusive to the U.S., as heightened consumption of these medications is reported in other nations such as the U.K. and Canada (Parekh, 2024a, 2024b). Furthermore, a recent report highlighted that the market size of ACE inhibitors is expected to reach US$ 11,831.7 million by 2030, up from US$ 8070.5 million in 2023 (Coherent Market Insights, 2023). Thus, the usage of CAP is anticipated to increase in the coming years.

The data above is remarkable since approximately 40–50 % of administered captopril is eliminated in its original form through urine, while the remaining portion undergoes transformation into disulfide and other metabolites (Mahmoud and Kümmerer, 2012). This process leads to a substantial occurrence of captopril in surface water, with concentrations reaching levels as elevated as 2.61 μg/L (Böger et al., 2020). While extensive data exists regarding the presence of various drugs in the environmental matrix and their toxic effects on aquatic species, there is a significant knowledge gap about CAP in these domains. To illustrate, our awareness is limited to three studies documenting CAP's toxic effects on hydrobionts. In the two first studies, authors reported a lethal concentration of 50 of >100, 168, 25, and 0.22 mg/L for *Daphnia manga*, *Desmodesmus subspicatus*, *Lemma minor*, and *Thamnocephalus platyurus*, respectively (Cleuvers, 2003; Nalecz-Jawecki and Persoone, 2006). Meanwhile, in the latest research, the authors observed that the presence of 1 μg/L, 1 mg/L, and 100 mg/L concentrations of CAP induced lipid damage and protein oxidation in the liver, brain, gills, kidney, and blood of *Cyprinus carpio* (Cortes-Diaz et al., 2017).

While previous studies have investigated the toxicological effects of CAP in different model systems, including its repercussions on aquatic organisms, a substantial knowledge deficit exists concerning its toxicity in fish, particularly zebrafish's early life stages. Zebrafish embryos undergo rapid and well-defined developmental processes, making them particularly vulnerable to disruptions caused by environmental stressors (Elizalde-Velázquez et al., 2021). Therefore, by assessing the impact of CAP on the embryonic development of zebrafish, it is possible to gain insights into potential adverse outcomes, such as deformities and mortality rates, which serve as vital indicators of ecotoxicity within fish populations. Considering this lack of information, the present study aimed to evaluate the influence of captopril on *Danio rerio*'s embryonic development. For this purpose, embryos were subjected to different concentrations of CAP (0.2–2000 μg/L), spanning previously reported in the environment extending to higher concentrations known to elicit toxic effects. By subjecting zebrafish embryos to a range of CAP concentrations, including those found in surface water, this study bridged the gap between laboratory-based toxicity assessments and real-world environmental conditions. This approach enabled a more accurate evaluation of the potential risks posed by CAP to freshwater fish populations and ecosystems. The postulated hypothesis suggested that the realistic concentrations of CAP (0.2 and 2 μg/L) would instigate oxidative stress and increase the expression of genes associated with apoptosis, thereby culminating in a considerable incidence of malformations and fatalities in embryos.

2. Method

2.1. Chemicals

CAP (CAS number: 62571-86-2) powder, with a minimum purity of 98 %, and all other reagents, unless specified otherwise, were procured from Sigma Aldrich (St. Louis, MO). A stock solution containing 20 mg/L of CAP was prepared using water as a solvent. Additionally, a secondary solution with a concentration of 2 mg/L was prepared from the stock solution. Aliquots from the stock solution were extracted to achieve 200 and 2000 μg/L concentrations in the subsequent experiments; meanwhile, aliquots from the secondary solution were extracted to achieve 2 and 0.2 μg/L concentrations.

2.2. Zebrafish maintenance

Zebrafish adults of the AB strain were housed at the Autonomous University of Mexico State (Mexico) within a 100 L open-water system. The system maintained a ratio of one zebrafish per liter of water, with a supply of aerated, dechlorinated, maintaining a temperature of 27 °C ± 1 °C and following a 10 h light - 14 dark cycle. The feeding regimen consisted of three daily sessions, providing Spirulina flakes (Ocean Nutrition, US) along with brine shrimp (*Artemia* sp. *nauplii*) to enhance the likelihood of spawning activity.

2.3. Embryo collection and exposure

The evening before the spawning event, a selection process was undertaken to allocate several mature zebrafish (4–5 cm) into different breeding chambers. Each chamber was designed to house 12 fish while maintaining a gender ratio of 2 females to 1 male. The initiation of light in the morning functioned as the stimulus for the spawning process. Oocytes were collected at 1 hour post-fertilization (hpf) and subsequently examined using a stereoscopic microscope (Zeiss Stemi 305) following the protocols outlined by Kimmel et al. (1995). Only those identified at the middle blastula stage (equivalent to 2.5 hpf) were isolated for incubation within a regulated environment (27 °C ± 1 °C) until they advanced to the sphere stage (4 hpf) (Fig. 1A). Upon reaching the 4 hpf stage, seventy-two embryos were chosen and allocated into 24-well plates, ensuring that each well accommodated one embryo. Each plate was spiked with either a control solution, comprising ultrapure water, or a test solution containing varying concentrations of CAP (0.2, 2, 200, and 2000 μg/L). Both the control solution and the solutions containing CAP were prepared using ultrapure water enriched with Instant Ocean (60 mg/L). Three 24-well plates were utilized for each test solution of CAP, as depicted in Fig. 1B ($n = 360$). Moreover, the exposure of embryos to each test solution of MET was conducted in triplicate across three distinct experiments ($n = 1080$). The determination of sample size adhered to the OECD 236 Guidelines, which specify the utilization of 24-well plates for conducting the test. Additionally, this study elected to employ three 24-well plates per treatment to ensure statistical significance. Randomization was conducted in the following manner. The total

number of embryos was divided into five groups, with 72 embryos allocated to each group, representing the control solution and each of the test solutions of CAP. Subsequently, all groups were assigned a number ranging from 1 to 5 using the standard INT(RAND()) function in Microsoft Excel. This numerical assignment to the groups designated the specific treatment the embryos were exposed to. The plates were maintained at a constant temperature of 27 °C ± 1 °C and adhered to a consistent light/dark cycle (14 hour light, 10 hour dark). A stereoscopic microscope (Zeiss Stemi 305, US) was employed at various time points (24, 48, 72, and 96 hour post-fertilization) during CAP exposure to evaluate embryo mortality and malformation rates. To acquire the samples of oxidative stress and gene expression, batches consisting of approximately 2000 zebrafish at the sphere stage (4 hpf) were apportioned in aquariums with a capacity of 5 L. The sample size considered the one documented by Nogueira et al., 2019. In their research, 700 unhatched zebrafish embryos were utilized at the initiation of each exposure for enzymatic determinations. Given the elevated mortality rates observed with CAP during the fish embryotoxicity test, this study employed 1000 embryos per test. Randomization proceeded as follows: Initially, the entire pool of embryos was partitioned into ten groups, each containing 1000 embryos (Fig. 1C). Subsequently, a numerical designation from 1 to 5 was allocated to each group employing the standard INT(RAND()) function in Microsoft Excel. This numerical allocation determined the treatment to which the embryos were exposed, with two groups assigned for each batch. Each batch was allocated one of the four concentrations of CAP treatment, with one batch designated for the control treatment. Throughout the exposure period, constancy in temperature (27 °C ± 1 °C) and light/dark cycles (14 h:10 h) was maintained across all batches. At 96 hpf, 1600 embryos (SD: ±85 embryos) were taken. Subsequently, half of these embryos were deposited into an Eppendorf tube filled with PBS, while the remaining half was placed in an Eppendorf tube containing RNALater (QIAGEN). 800 embryos (SD: ±42 embryos) were utilized to carry out each test, as depicted in Fig. 1D (n = ~8000). Moreover, each test was conducted in triplicate across three distinct experiments (n = ~ 24,000).

2.4. Oxidative stress assessment

A rotor-stator homogenizer was utilized to homogenize the tissue, acquiring two tubes for each homogenized sample. In the initial tube, a

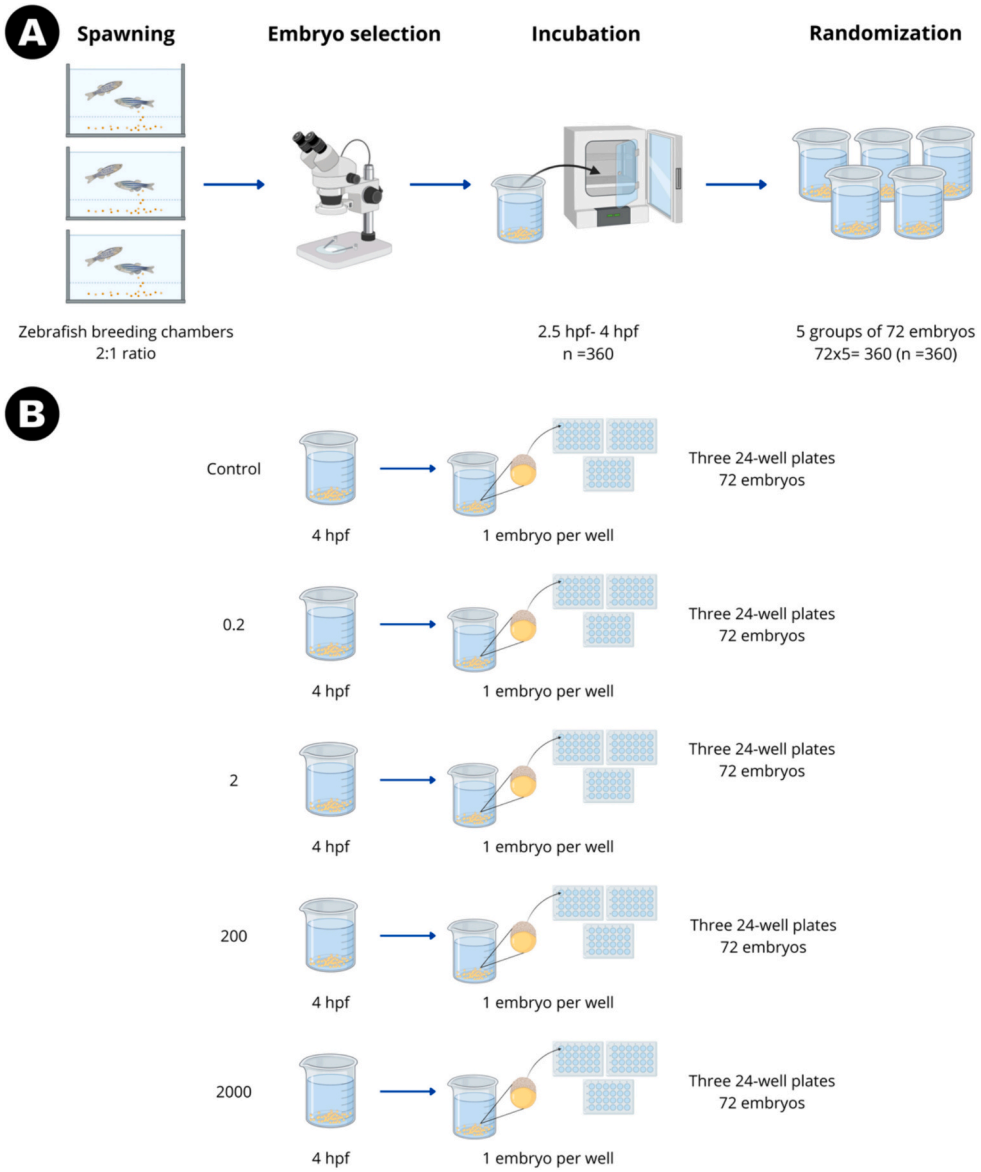

Fig. 1. Experimental design of captopril's influence on *Danio rerio* embryonic development. **A–B)** Embryo collection and zebrafish embryo toxicity test. **C–D)** Embryo collection and sampling for oxidative stress and gene expression assays. The experimental design was replicated three times in three independent experiments.

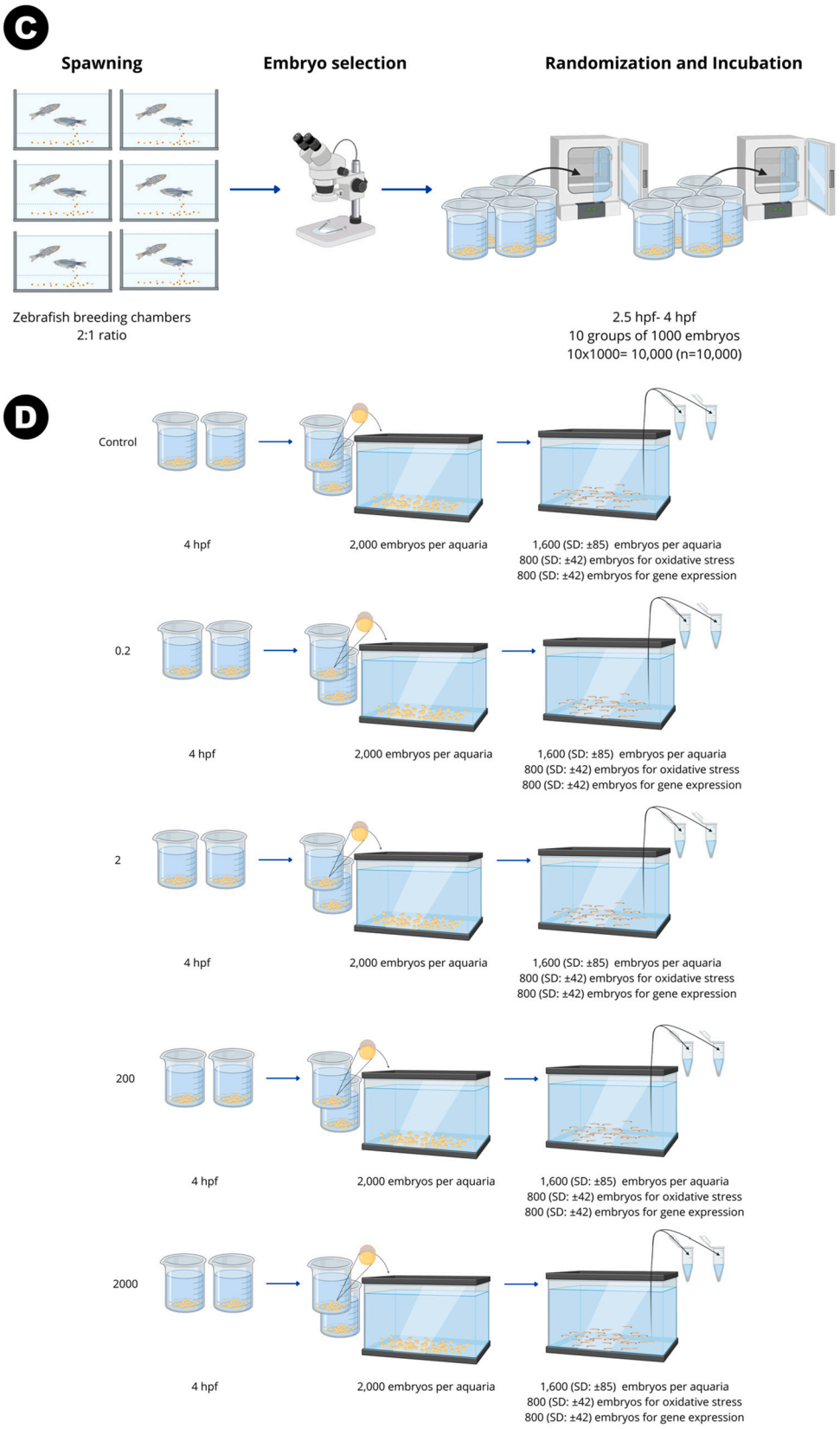

Fig. 1. (*continued*).

mixture of 300 μL homogenate and 300 μL of 20 % trichloroacetic acid were centrifuged at 11495 rpm and 4.0 °C for 15 min. The resultant precipitate was then employed to quantify carbonylated proteins (PCC) content following the methodology described by Levine et al. in 1994. Simultaneously, the supernatant was utilized to assess the levels of lipoperoxidation (LPX) and hydroperoxides (HPC) using the protocols

outlined by Buege and Aust in 1978 and Jiang et al. in 1992, respectively. For the second tube, 700 μL of homogenate underwent centrifugation at 12,500 rpm and 4.0 °C for 15 min. The resulting supernatant was employed for the determination of superoxide dismutase (SOD) and catalase (CAT), following the procedures outlined by Misra and Fridovich in 1972 and Radi et al. in 1991, respectively. All biomarker results were standardized using the Bradford method, as detailed by Bradford in 1976. For an in-depth description of the above guidelines, refer to supplementary material.

2.5. Gene expression evaluation

The process of RNA isolation for each tissue sample involved using the RNeasy Mini Kit provided by QIAGEN. Subsequently, in a sterile Eppendorf tube devoid of RNases, a mixture was prepared by combining 2.0 μL of 7× gDNA Wipeout Buffer, 10.0 μL of the RNA template, and 2.0 μL of RNase-free water. Following a 2-minute incubation at 42 °C and immediate cooling on ice, 1.0 μL of Quantiscript reverse transcriptase, 4.0 μL of Quantiscript RT Buffer 5×, and 1.0 μL of RT Primer Mix were added to the mixture. The resulting blend underwent an incubation process at 42 °C for 15 s, followed by a subsequent incubation at 93 °C for 3 min to facilitate the inactivation of reverse transcription. The qPCR reaction was initiated by combining 25 μL of the 2× QuantiTect SYBR Green PCR (QIAGEN), 1.0 μL of each primer, 4.0 μL of cDNA, and 19 μL of RNase-free water. The genes under evaluation are detailed in Table 1. The qPCR was executed under specific conditions: an initial denaturation step at 94 °C for 10 min, followed by 35 cycles of denaturation at 94 °C for 15 s, primer annealing for 30 s, and extension at 72 °C for 30 s. Post the qPCR amplification cycles, a dissociation curve analysis was conducted with parameters including a preliminary denaturation step at 95 °C for 10 s, followed by a temperature reduction to 65 °C for 10 s and subsequent re-elevation to 95 °C for 10 s, with increments of 0.2 °C. This meticulous procedure aimed to discern specific from non-specific products within the samples. Data points were collected at each increment of the melting curve, and negative controls were integrated to validate the results using samples devoid of template, with RNase-free water acting as the substitute. The 2− Δ ΔCq method (Pfaffl, 2001; Pfaffl et al., 2002; Schmittgen and Livak, 2008) was applied to calculate mRNA expression changes. The Gene Q Rotor (QIAGEN) served as the qPCR equipment, and the β-actin gene was employed to normalize the expression of target genes.

Table 1
Nucleotide sequences of the primers designed for the (qRT-PCR) analysis.

Gen	Forward, reverse	Primer sequence (5′ → 3′)	Access number
bax	F	GGC TAT TTC AAC CAG GGT TCC	AF231015
	R	TGC GAA TCA CCA ATG CTG T	
bcl2	F	TAC GGG ATG CTG GAG ATG AA	NM_001030253
	R	CCC AGT TCA CTC CGT CTC TA	
p53	F	GCG GAT TTG CTT TGT GGA TG	NM_001271820
	R	CCG ACC TCC TCT CCA CTA AA	
casp3	F	GATGAACGGAGACTGTGTGG	NM_131877.3
	R	CTGAAGGCATGGGATTGAGG	
tbx2a	F	ACGTTTTCCCTGAGACCGATT	AF179405
	R	ATGGAAGGGTCAGCTGTTTCC	
tbx2b	F	ACGTTTTCCCTGAGACCGATT	NM_131051
	R	ATGGAAGGGTCAGCTGTTTCC	
irx3b	F	CATGTCTCTCCCGCAGCTAG	NM_213100
	R	TCAGCTGGTTGAGAACGGAC	
slc12a1	F	GCGTGCCCAAACCCTGATTTT	XM_021467734.1
	R	GCCAAATTTGACCACACCCC	
kcnj1	F	TCCCGTATCTTCTGGGGTGGT	NM_001045176.1
	R	GTTGATGCTGACCTGGTCCA	

bax: B-cell lymphoma 2-associated X protein; ***bcl2:*** B-cell lymphoma 2; ***p53:*** cellular tumor antigen p53; ***caps3:*** caspase 3; ***tbx2a:*** T-Box transcription factor 2a; ***tbx2b:*** T-Box transcription factor 2b; ***irx3b:*** iroquois homeobox 3b; ***slc12a1:*** solute carrier family 12 member 1; ***kcnj1:*** potassium inwardly rectifying channel subfamily J member 1.

2.6. CAP quantification

During the zebrafish embryo toxicity test, 140 μL of water from 72 wells were gathered and combined for each treatment group, resulting in combined water samples of 10.8 mL for each CAP test solution. For the oxidative stress study, 10 mL of water were collected from each of the five lots and stored at −20 °C until quantification. Sampling for both experiments took place at 0 and 96 hpf. Measurements were taken from water samples from all three experiments to verify exposure. Aliquots of 2.5 μL were extracted at both 0 and 96 hpf and subsequently combined with 2.5 μL of a 60 μM internal standard solution and with 7.5 μL of a 0.5 % formic acid solution. The formic acid solution (0.1 %) served to quench the reaction and also to make the1/5th dilution of the reaction mixture. Analysis was performed using the Agilent 1260 liquid chromatograph coupled with API 5500 Qtrap MS. 5.0 μL of each sample were injected into the system for analysis. Separation involved reverse phase HPLC with a Phenomenex Jupiter C-18 column (50 mm length, 1 mm i.d., 5.0 μm particle size) at 25 °C. The mobile phase consisted of water with 1 % formic acid (FA) as solvent A and acetonitrile with 1 % FA as solvent B. The flow rate was optimized at 0.4 mL/min, with 5 out of 7 parameters optimized using statistical software "Design Expert V9.0." The final values were: gas temperature 300 °C, gas flow 12 L/min, nebulizer pressure 30 psi, sheath gas heater 240 °C, sheath gas flow 10 L/min, capillary voltage 3000 V, and nozzle voltage (V Charging) 1000 V. Collision energy and fragmentor voltages were set at 20 eV and 100 V, respectively. A calibration curve with five points was created by adding CAP to ultrapure water, with concentrations ranging from 0.005 to 4000 μg/L.

2.7. Statistical analysis

Homoscedasticity was verified using Bartlett tests, and the assessment of normality was carried out via the Shapiro-Wilk test. Mean differences were ascertained using the Tukey test, with a significance threshold set at $p < 0.05$. A one-way ANOVA test, performed using Sigma Plot 12.3 software at a significance level of $\alpha = 0.05$, was employed to scrutinize differences among treatment groups. The presentation of results for all experiments followed the format of mean ± standard deviation (SD). To gauge the correlation strength among oxidative stress, gene expression, and malformation and mortality rates, a Pearson correlation analysis was conducted with a pre-established significance level of $p < 0.05$. Following this, the established correlation was visually represented using a chord correlation.

3. Results

3.1. CAP quantification

The concentrations of CAP in the water samples aligned with the nominal values. Table 2 illustrates a time-dependent decrease in CAP concentrations in both experiments. Additionally, the control group exhibited CAP concentrations below the quantification limit. The analyses of the results were conducted based on nominal values, as CAP concentration remained above 80 % in all samples.

3.2. Mortality and teratogenic effects

Embryos subjected to CAP exhibited malformations and mortality. Nevertheless, varying rates of these adverse effects were noted across all treatments. For instance, the embryos exposed to 2000 μg/L of CAP showed the highest incidence of mortality and malformations, followed by concentrations of 200, 2.0, and 0.2 μg/L in descending order (Fig. 2). Concurrent with the mortality and malformation rates, the severity of malformations in the embryos displayed a concentration-dependent

Table 2
Measured concentrations of CAP in both the *Danio rerio* embryo toxicity test and oxidative stress test.

Nominal concentrations	Measured concentrations (μg/L)	
	0 hpf	96 hpf
Zebrafish embryo toxicity test		
Control	<LOQ	<LOQ
0.2 μg/L	0.21 ± 0.01	0.17 ± 0.02
2 μg/L	2.04 ± 0.05	1.69 ± 0.03*
200 μg/L	200.00 ± 0.37	173.49 ± 1.51*
2000 μg/L	2000.18 ± 0.96	1720.15 ± 5.38*
Oxidative stress test		
Control	<LOQ	<LOQ
0.2 μg/L	0.19 ± 0.01	0.16 ± 0.01*
2 μg/L	2.00 ± 0.02	1.67 ± 0.09*
200 μg/L	201.36 ± 0.84	167.12 ± 2.36*
2000 μg/L	2000.95 ± 1.08	1681.39 ± 8.44*

Values represent mean ± standard deviation of each concentration. LOQ: limit of quantification (10.72 ng/L ng/L). LOD: limit of detection (5.91 ng/L).
* Denotes a significant difference compared to the nominal concentrations ($p < 0.05$). Zebrafish embryo toxicity test: $F(4,40) = 11.595156$; $p < 0.001$. Oxidative stress test: $F(4,40) = 49.819585$; $p < 0.001$.

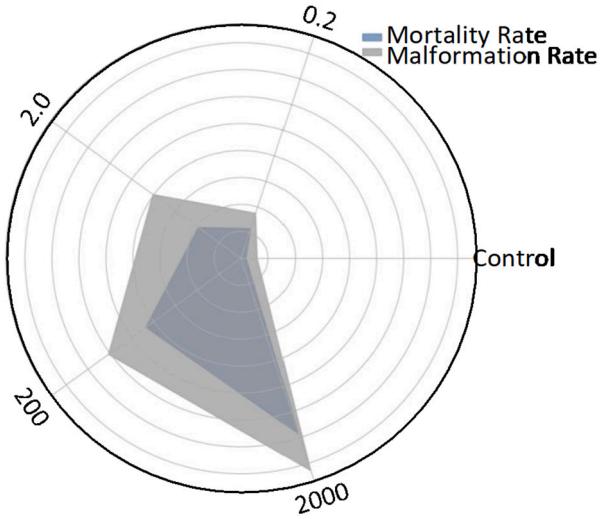

Fig. 2. Mortality and malformation rates of *Danio rerio* embryos exposed to CAP (μg/L) depicted in radial charts. The data is represented as means ± standard deviation (S.D) derived from three independent experiments.

escalation. Consequently, embryos exposed to 2000 μg/L demonstrated the most severe malformations, whereas those subjected to 0.2 μg/L exhibited milder malformations (Fig. 4). Overall, the observed malformations in embryos comprised tail malformation, scoliosis, pericardial edema, yolk sac deformation, and craniofacial malformation. However, pericardial edema emerged as the predominant malformation observed consistently across all administered treatments (Fig. 3). The embryos within the control group also exhibited occurrences of specific malformations, namely scoliosis and tail deformation. Nevertheless, it is crucial to emphasize that these malformations were not statistically significant, given that the malformation rate remained below 5 % in all replicates.

3.3. Oxidative stress

Embryonic exposure to CAP induced significant alterations in all oxidative stress biomarkers when compared to the control group (SOD: $F(4,40) = 72.830983$; $p < 0.001$) (CAT: $F(4,40) = 105.126371$; $p < 0.001$) (LPX: $F(4,40) = 10{,}061.626748$; $p < 0.001$) (PCC: $F(4,40) = 124.134313$; $p < 0.001$) (HPC: $F(4,40) = 109.517657$; $p < 0.001$). However, response variations are evident among antioxidant enzymes and oxidative damage biomarkers. Superoxide dismutase (SOD) and catalase (CAT) activities, for instance, exhibited a concentration-dependent increase up to the third concentration of CAP. Unexpectedly, in the highest concentration, the antioxidant activity of SOD demonstrated a significant decrease compared to the other treatments, except for the control group (Fig. 5A). In contrast to SOD, CAT displayed a substantial decline in activity even when compared to the control group (Fig. 5B). Regarding oxidative damage biomarkers, lipid peroxidation (LPX), hydroperoxide content (HPC), and protein carbonyl content (PCC), there was a concentration-dependent increase across all exposure concentrations. All these biomarkers exhibited a concentration-dependent increase and no evidence of a decline in any treatment.

3.4. Gene expression

Substantial alterations were noted in the expression patterns of genes associated with apoptosis, namely bax ($F(4,40) = 90.967947$; $p < 0.001$), bcl2 ($F(4,40) = 91.572568$; $p < 0.001$), p53 ($F(4,40) = 104.385742$; $p < 0.001$; $p < 0.001$), and casp3 ($F(4,40) = 83.940286$; $p < 0.001$), as well as those linked to organogenesis, including tbx2a ($F(4,40) = 110.855774$; $p < 0.001$), tbx2b ($F(4,40) = 67.622462$; $p < 0.001$), and irx3b ($F(4,40) = 19.010989$; $p < 0.001$), and ion exchange, such as slc12a1 ($F(4,40) = 92.811878$; $p < 0.001$) and kcnj1 ($F(4,40) = 54.773624$; $p < 0.001$) (Fig. 6). Distinct trends in gene expression were evident, with a notable increase observed in genes associated with apoptosis across all treatments. Meanwhile, genes linked to organogenesis and ion exchange exhibited a significant decrease in expression. All the above-described alterations were concentration-dependent.

3.5. Pearson correlation

The Pearson correlation analysis revealed that all biomarkers, except for SOD and CAT, exhibited robust and positive correlations with both mortality and malformation rates (Fig. 7). In addition, it is essential to note that the analysis demonstrated a significant and positive correlation between apoptosis-related genes and those associated with organogenesis, as well as oxidative damage biomarkers. SOD and CAT exhibited a minimal correlation with all biomarkers.

4. Discussion

To address the substantial knowledge deficit about the toxic effects of CAP on aquatic species, this investigation sought to assess the potential impact of varying concentrations of CAP (ranging from 0.2 to 2000 μg/L) on the embryonic development of *Danio rerio*. Based on the findings, CAP demonstrated the potential to elicit malformations in *Danio rerio* embryos across the investigated range of concentrations (0.2, 2, 200, and 2000 μg/L). These malformations encompassed pericardial edema, craniofacial abnormalities, scoliosis, tail deformation, and yolk sac distortion. To the best of our knowledge, this study represents the first investigation addressing the toxic effects of CAP at environmentally pertinent concentrations. Nevertheless, a few preceding articles have already documented the potential teratogenic effects of CAP in *Danio rerio* embryos. In another study, for instance, the authors pointed out that CAP, within the concentration range of 1000 to 20,000 μM, did not manifest teratogenic effects at 2 days post-fertilization (pdf). However, they noted the emergence of teratogenic effects at 4 dpf (Cendoya et al., 2020). Concordantly with these results, Westhoff et al., 2013 indicated that 40 mM of CAP increased the edema formation and altered the morphological structure of pronephros in *Danio rerio* embryos (Westhoff et al., 2013). In many vertebrates, including zebrafish, the pronephros is a transient structure that forms during the early stages of embryonic development but is replaced by more functional kidneys as the embryo

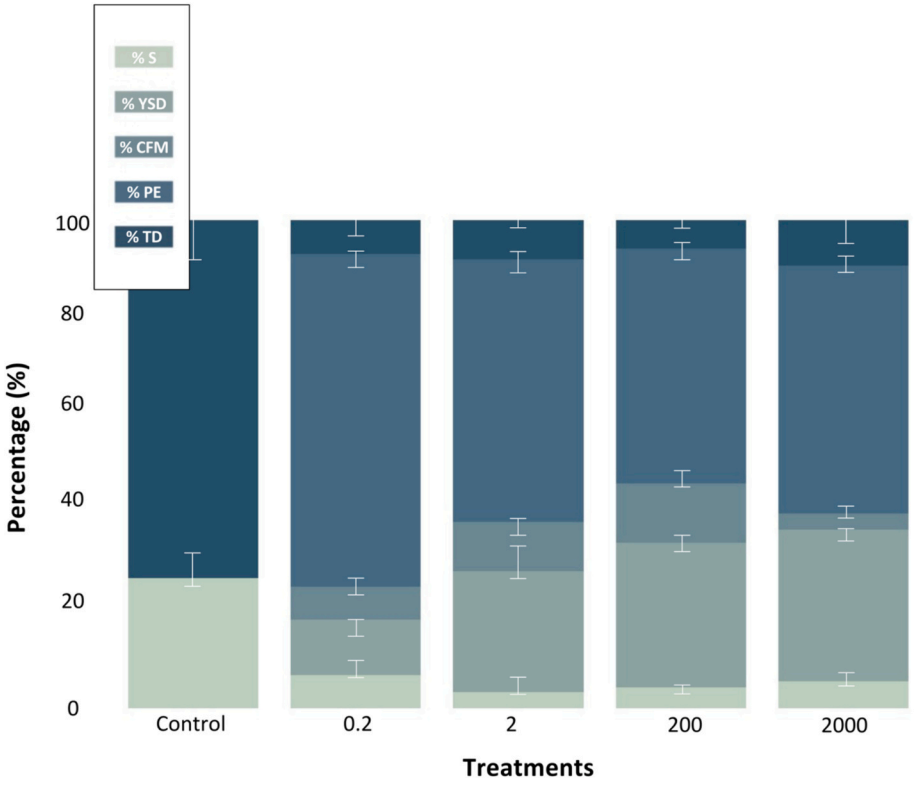

Fig. 3. Cumulative incidence of specific malformations observed in *Danio rerio* embryos following exposure to CAP, presented as percentages. The data is represented as means ± standard deviation (S.D) derived from three independent experiments. **DT:** malformation of tail; **S:** scoliosis; **PE:** pericardial edema; **YSD:** yolk sac deformation; **CFM:** craniofacial malformation.

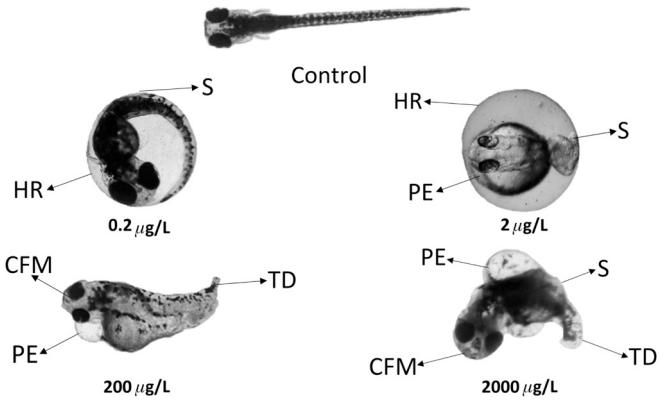

Fig. 4. Main malformations produced by CAP in *Danio rerio* embryos. **DT:** malformation of tail; **S:** scoliosis; **PE:** pericardial edema; **YSD:** yolk sac deformation; **CFM:** craniofacial malformation.

matures (Naylor et al., 2017). The above is noteworthy as morphological defects within the zebrafish pronephros may be causally linked to diminished renal function and manifest as pericardial edema, kidney cysts, hydrocephalus of the brain, or curvature of the body (Nguyen et al., 2023). Hence, the observed pericardial edema and scoliosis herein might have arisen due to dysfunction in the pronephros of zebrafish. To substantiate the statement above, an evaluation of gene expression was undertaken for irx3b, tbx2a, and tbx2b in this study. irx3b assumes a pivotal function in the maturation of the distal tubule within the pronephros, the morphogenesis of the pronephric duct, and the specialization of epithelial cells within the pronephric nephron tubule (Wingert and Davidson, 2011). Simultaneously, tbx2a and tbx2b contribute to the development of animal organs, the migration of cells during gastrulation, and the determination of photoreceptor cell fate (Alvarez-Delfin et al., 2009; Sedletcaia and Evans, 2011; Thi Thu et al., 2013). Nevertheless, it is crucial to underscore that Drummond et al., 2017 also discerned significant roles for the transcription factors tbx2a and tbx2b in the advanced stages of distal development (Drummond et al., 2017). Consequently, as observed in this study, a reduction in the expression of these transcription factors could result in adverse effects on pronephric development and functionality and ultimately contribute to the initiation of kidney disease.

While CAP is not directly linked to the onset of renal disease, it is noteworthy that ACE inhibitors, including CAP, can diminish aldosterone levels by inhibiting the conversion of angiotensin I to angiotensin II (Kim et al., 2016). Aldosterone, a mineralocorticoid hormone, influences the late distal tubule and collecting duct of nephrons within the kidney, promoting sodium and water reabsorption while facilitating potassium excretion (Scott et al., 2017). Prolonged disruptions in sodium and potassium equilibrium, particularly when inadequately addressed, may contribute to the advancement of renal disease (Kovesdy, 2014; Soi and Yee, 2017). Likewise, persistent disturbances in water balance can induce alterations in extracellular fluid volume, potentially exacerbating renal damage and edema formation (Prowle et al., 2010). Apart from evaluating the gene expression of irx3b, tbx2a, and tbx2b, an assessment was conducted on the expression of two genes linked to ion transmembrane transport. slc12a1 and kcnj1, two genes expressed in the renal system and the pronephric duct, play crucial roles in maintaining cell volume homeostasis, inorganic ion homeostasis, and facilitating inorganic ion transmembrane transport. The results indicated that exposure to CAP alters the gene expression of slc12a1 and kcnj1 in *Danio rerio* embryos, suggesting this drug can prompt early kidney damage. An additional plausible mechanism through which the transmembrane transport of ions may be modified is oxidative stress. Some authors, for instance, have posited that the membrane assault by free radicals can concomitantly induce disorder in the lipid bilayer and

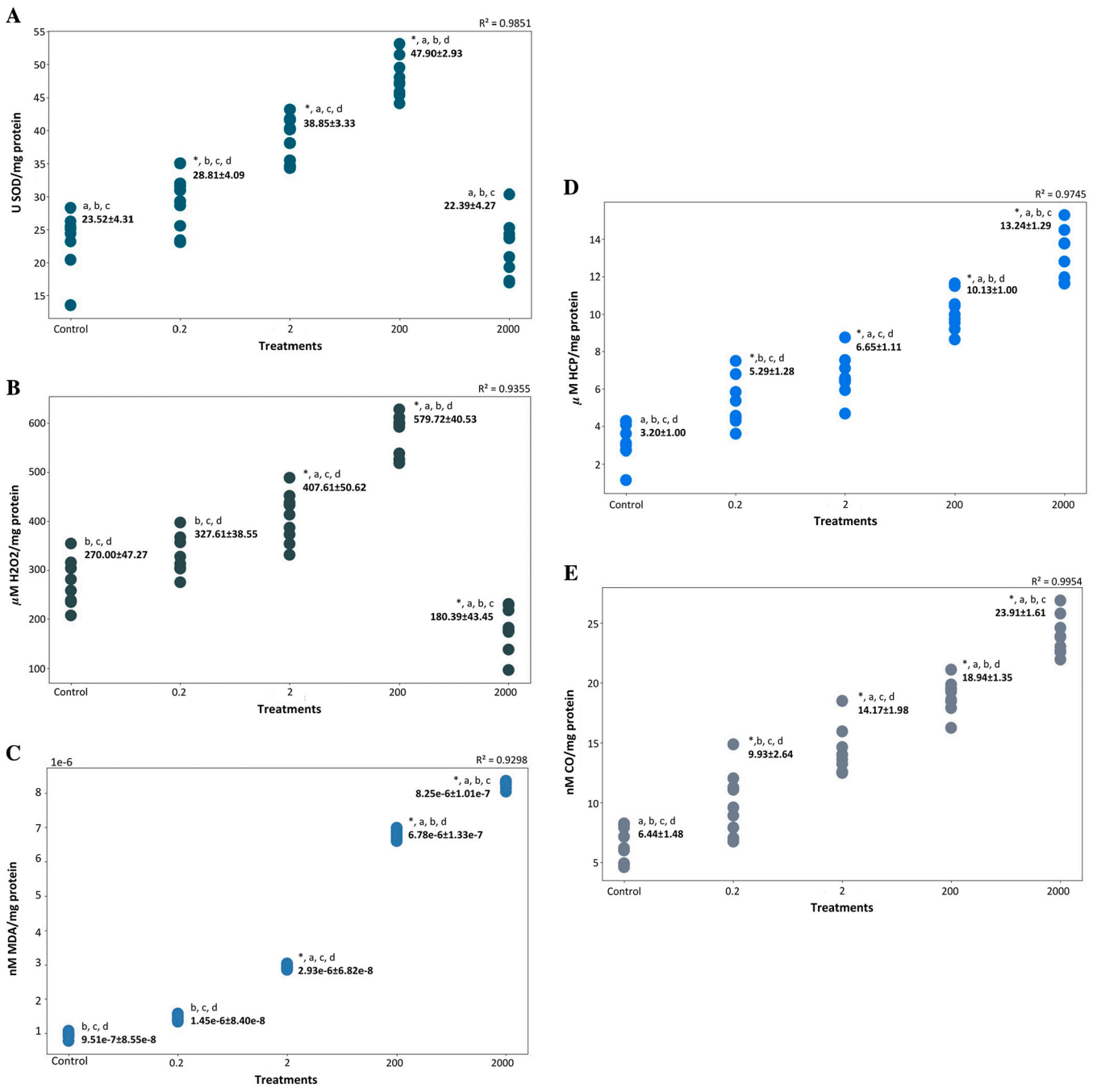

Fig. 5. Oxidative stress alterations in *Danio rerio* embryos exposed to CAP. The data is represented as means ± standard deviation (S·D) derived from three independent experiments. **A:** SOD; **B:** CAT, **C:** LPX; **D:** HPC; **E:** PCC. * denotes a significant difference compared to the control group ($p < 0.05$). a denotes a significant difference compared to the 0.2 μg/L treatment ($p < 0.05$). b denotes a significant difference compared to the 2 μg/L treatment ($p < 0.05$). c denotes a significant difference compared to the 200 μg/L treatment ($p < 0.05$). d denotes a significant difference compared to the 2000 μg/L treatment ($p < 0.05$). **SOD:** superoxide dismutase; **CAT:** catalase; **LPX:** lipoperoxidation; **HPC**: hydroperoxides; **PCC:** carbonylated proteins content.

suppress the activity of Na/K-ATPase (Dobrota et al., 1999). Furthermore, free radicals can directly instigate posttranslational modifications in ion channels or indirectly influence channel functionality by impacting the signaling pathways regulating gene transcription, trafficking, and turnover (Ramírez et al., 2016). Herein, the findings demonstrated that exposure to CAP resulted in oxidative stress in *Danio rerio* embryos. This suggests that the drug can directly or indirectly disrupt ion transmembrane transport, thereby contributing to the development of malformations in the embryos.

Both disruption of ion transmembrane transport and oxidative equilibrium have been reported to be determinants in both the activation and progression of the apoptotic cascade (Kondratskyi et al., 2015; Yang et al., 2017). Multiple research investigations, for instance, have illustrated the participation of distinct ion conduits in overseeing essential cellular activities, like cell proliferation and programmed cell death. This encompasses channels in the cell membrane and within the cell, comprising potassium, calcium, sodium, and chloride channels, and store-operated calcium channels (Saha et al., 2016; Busschaert et al., 2017; Bortner and Cidlowski, 2020). In addition, some researchers, such as Chen et al. (2022), have illustrated that elevated levels of reactive oxygen species (ROS) and the activation of various signaling pathways result in upregulating bax and caspase-3. In agreement with this study,

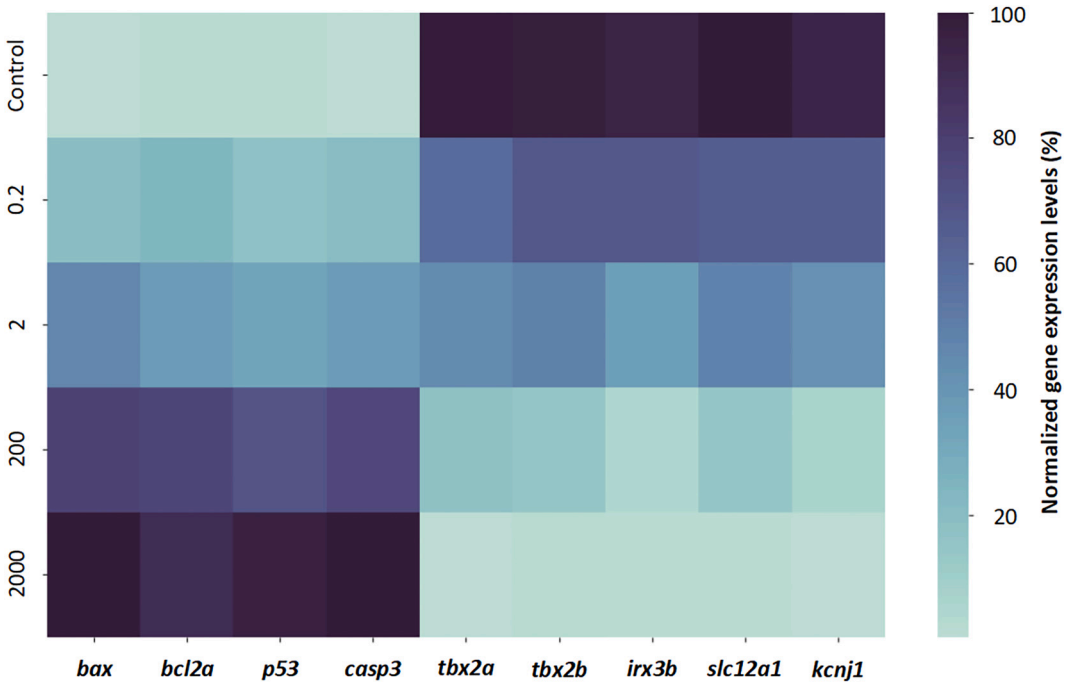

Fig. 6. Expression levels of genes associated with apoptosis (*bax, bcl2, p53, and casp3*), organogenesis (*tbx2a, tbx2b, and irx3b*), and ion exchange (*slc12a1 and kcnj1*) in *Danio rerio* embryos following exposure to CAP. ***bax:*** B-cell lymphoma 2-associated X protein; ***bcl2:*** B-cell lymphoma 2; ***p53:*** cellular tumor antigen p53; ***caps3:*** caspase 3; ***tbx2a:*** T-Box transcription factor 2a; ***tbx2b:*** T-Box transcription factor 2b; ***irx3b:*** iroquois homeobox 3b; ***slc12a1:*** solute carrier family 12 member 1; ***kcnj1:*** potassium inwardly rectifying channel subfamily J member 1.

our investigation showed that CAP heightened bax, bcl2, casp3, and p53 expression levels within the embryos. Proteins belonging to the Bcl-2 family, namely Bax and Bcl-2, play a crucial role in controlling apoptosis. The pro-apoptotic protein, Bax, triggers cell demise by creating pores in the outer mitochondrial membrane, causing the liberation of cytochrome *c* (Zhang et al., 2017). Conversely, the anti-apoptotic protein, Bcl-2, hinders cell death by blocking the release of cytochrome *c* and preserving the integrity of the mitochondrial membrane(Kalkavan and Green, 2018). Acting as a tumor suppressor, p53 functions as a transcription factor, monitoring DNA integrity during cell division. In response to DNA damage, p53 can pause the cell cycle for repair or initiate apoptosis if the damage is irreparable (Kastenhuber and Lowe, 2017). Caspase-3, an enzyme in the execution phase of apoptosis, is activated by various signals, including those from p53. Once activated, caspase-3 cleaves and activates other proteins, orchestrating the controlled breakdown of cellular components (Asadi et al., 2022). Together, p53 and caspase-3 play crucial roles in safeguarding genomic integrity, regulating the cell cycle, and executing programmed cell death to eliminate damaged or unwanted cells. In conclusion, the observations above indicate that oxidative stress induced by CAP, coupled with alterations in ion transmembrane dynamics, may initiate a cascade of detrimental reactions, culminating in the formation of malformations and, in severe cases, embryonic fatality.

Finally, the authors would like to acknowledge that reported toxic effects may not fully reflect the extent of toxicity experienced by the organisms or systems under investigation. Reporting nominal concentrations for the harmful effects, as occurred herein, may underestimate the actual toxicity observed in the study. The above is because the concentrations of substances in the exposure solutions may have declined over time due to degradation, absorption, or other processes. Considering potential limitations associated with substance concentrations is crucial when interpreting toxicological data and drawing conclusions regarding the effects of environmental contaminants on ecosystems or human health.

5. Conclusions

This research represents the first study of CAP's toxic effects at environmentally relevant concentrations, expanding our understanding of its impact on aquatic organisms. While previous studies have highlighted the teratogenic effects of CAP on *Danio rerio* embryos, this research delves into the molecular mechanisms underlying these effects. Gene expression analysis revealed a reduction in *irx3b, tbx2a, and tbx2b*, critical genes associated with pronephric development. Dysregulation of these genes may contribute to kidney-related issues, as well as edema and scoliosis formation in zebrafish. Furthermore, this study investigated the indirect impact of CAP on renal health, considering its role as an ACE inhibitor. Although CAP itself is not directly linked to renal disease, its influence on aldosterone levels and subsequent disturbances in sodium and potassium equilibrium may contribute to renal damage. Evaluation of genes involved in ion transmembrane transport, such as *slc12a1 and kcnj1*, indicated that CAP exposure alters their expression, suggesting early kidney damage. The findings herein also shed light on the potential role of oxidative stress induced by CAP in disrupting ion transmembrane transport, leading to malformations in embryos. This disruption, coupled with alterations in the apoptotic cascade, as evidenced by increased expression of *bax, bcl2, casp3, and p53,* suggests a cascade of detrimental reactions that could culminate in malformations and embryonic fatality. The present study emphasizes the need for a holistic understanding of the molecular pathways involved in CAP onset of toxicity in aquatic species.

CRediT authorship contribution statement

Fernando García-Valdespino: Methodology, Data curation. **Gustavo Axel Elizalde-Velázquez:** Writing – original draft, Supervision, Investigation, Formal analysis, Data curation, Conceptualization. **Selene Elizabeth Herrera-Vázquez:** Software, Investigation, Formal analysis, Data curation. **Leobardo Manuel Gómez-Oliván:** Writing – review & editing, Writing – original draft, Visualization, Supervision,

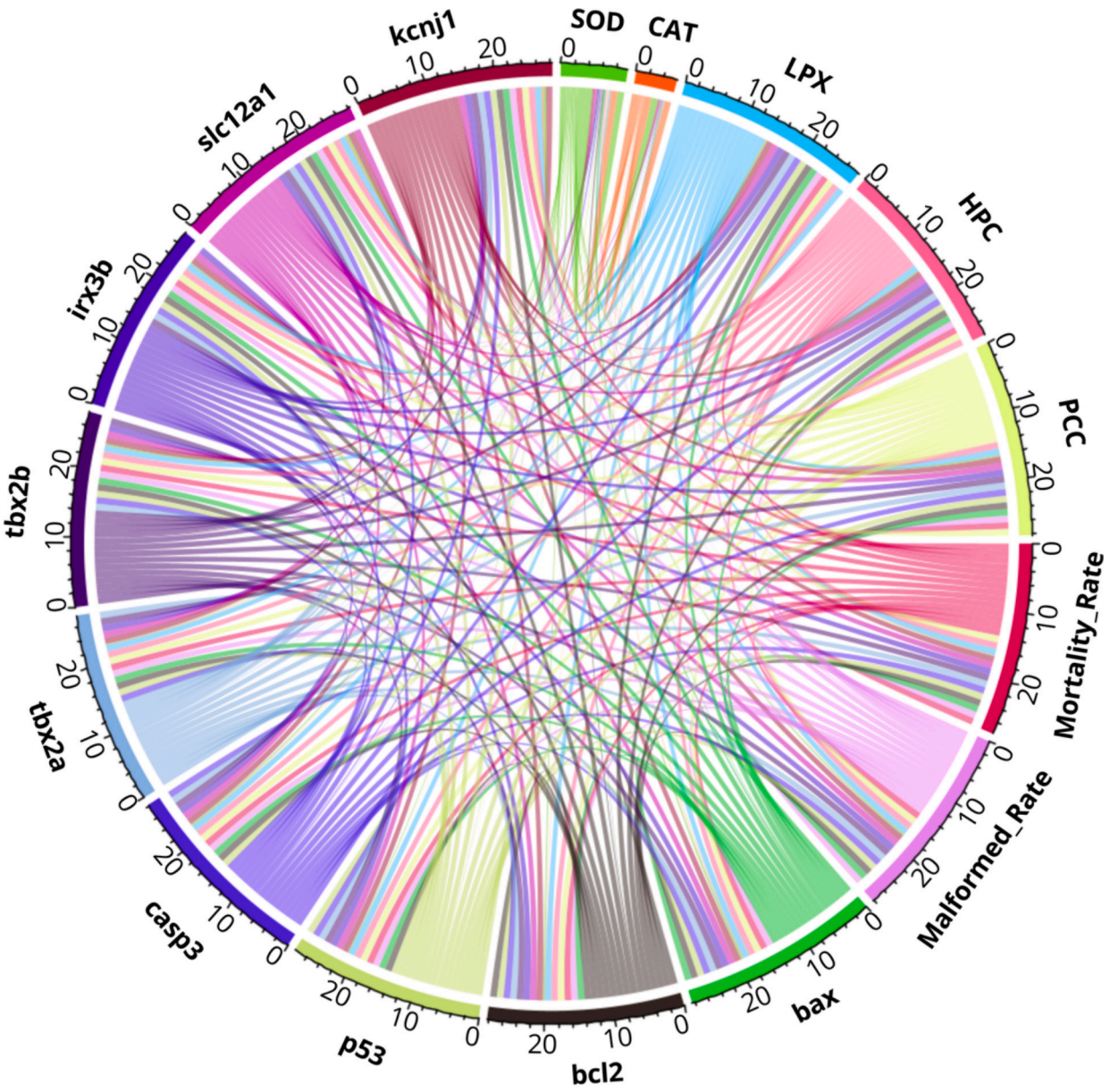

Fig. 7. Pearson correlation among oxidative stress and gene expression biomarkers, alongside malformation rate and mortality rate in embryos of *Danio rerio*. ***bax:*** B-cell lymphoma 2-associated X protein; ***bcl2:*** B-cell lymphoma 2; ***p53:*** cellular tumor antigen p53; ***caps3:*** caspase 3; ***tbx2a:*** T-Box transcription factor 2a; ***tbx2b:*** T-Box transcription factor 2b; ***irx3b:*** iroquois homeobox 3b; ***slc12a1:*** solute carrier family 12 member 1; ***kcnj1:*** potassium inwardly rectifying channel subfamily J member 1. **SOD:** superoxide dismutase; **CAT:** catalase; **LPX:** lipoperoxidation; **HPC**: hydroperoxides; **PCC:** carbonylated proteins content.

Resources, Project administration, Investigation, Formal analysis, Conceptualization.

Declaration of competing interest

The authors declare that they have no known competing financial interests or personal relationships that could have appeared to influence the work reported in this paper.

Data availability

Data will be made available on request.

Acknowledgments

This study was made possible by financial support from the Secretaría de Investigación y Estudios Avanzados de la Universidad Autónoma del Estado de México, Mexico (6982/2024CIB).

Appendix A. Supplementary data

Supplementary data to this article can be found online at https://doi.org/10.1016/j.scitotenv.2024.173179.

References

Alvarez-Delfin, K., Morris, A.C., Snelson, C.D., Gamse, J.T., Gupta, T., Marlow, F.L., Fadool, J.M., 2009. Tbx2b is required for ultraviolet photoreceptor cell specification during zebrafish retinal development. Proc. Natl. Acad. Sci. 106 (6), 2023–2028.

Asadi, M., Taghizadeh, S., Kaviani, E., Vakili, O., Taheri-Anganeh, M., Tahamtan, M., Savardashtaki, A., 2022. Caspase-3: structure, function, and biotechnological aspects. Biotechnol. Appl. Biochem. 69 (4), 1633–1645.

Böger, B., Vilhena, R., Fachi, M., Concentino, V., Junkert, A., Santos, J., Domingos, E., Zamora, P., Pontarolo, R., 2020. HPLC-MS/MS method for quantification of pharmaceuticals in subtropical rivers and water treatment plants in Brazil. Journal of Environmental Science and Public Health 4 (4), 390–408.

Bortner, C.D., Cidlowski, J.A., 2020. Ions, the movement of water and the apoptotic volume decrease. Frontiers in cell and developmental biology 8, 611211.
Busschaert, N., Park, S.H., Baek, K.H., Choi, Y.P., Park, J., Howe, E.N., Shin, I., 2017. A synthetic ion transporter that disrupts autophagy and induces apoptosis by perturbing cellular chloride concentrations. Nat. Chem. 9 (7), 667–675.
Cendoya, X., Quevedo, C., Ipiñazar, M., Planes, F.J., 2020. Computational approach for collection and prediction of molecular initiating events in developmental toxicity. Reprod. Toxicol. 94, 55–64.
Chen, L., Tao, D., Yu, F., Wang, T., Qi, M., Xu, S., 2022. Cineole regulates Wnt/β-catenin pathway through Nrf2/keap1/ROS to inhibit bisphenol A-induced apoptosis, autophagy inhibition and immunosuppression of grass carp hepatocytes. Fish Shellfish Immunol. 131, 30–41.
Cleuvers, M., 2003. Aquatic ecotoxicity of pharmaceuticals including the assessment of combination effects. Toxicol. Lett. 142 (3), 185–194.
Coherent Market Insights, 2023. Angiotensin converting enzymes (ACE) inhibitors market size & share analysis - industry research report - growth trends. https://www.coherentmarketinsights.com/market-insight/angiotensin-converting-enzymes-ace-inhibitors-market-2746.
Cortes-Diaz, M.J.A., Rodríguez-Flores, J., Castañeda-Peñalvo, G., Galar-Martínez, M., Islas-Flores, H., Dublán-García, O., Gómez-Oliván, L.M., 2017. Sublethal effects induced by captopril on Cyprinus carpio as determined by oxidative stress biomarkers. Sci. Total Environ. 605, 811–823.
Dobrota, D., Matejovicova, M., Kurella, E.G., Boldyrev, A.A., 1999. Na/K-ATPase under oxidative stress: molecular mechanisms of injury. Cell. Mol. Neurobiol. 19, 141–149.
dos Santos, A.J., Cabot, P.L., Brillas, E., Sirés, I., 2020. A comprehensive study on the electrochemical advanced oxidation of antihypertensive captopril in different cells and aqueous matrices. Appl. Catal. Environ. 277, 119240.
Drummond, B.E., Li, Y., Marra, A.N., Cheng, C.N., Wingert, R.A., 2017. The tbx2a/b transcription factors direct pronephros segmentation and corpuscle of Stannius formation in zebrafish. Dev. Biol. 421 (1), 52–66.
Elizalde-Velázquez, G.A., Gómez-Oliván, L.M., Islas-Flores, H., Hernández-Navarro, M. D., García-Medina, S., Galar-Martínez, M., 2021. Oxidative stress as a potential mechanism by which guanylurea disrupts the embryogenesis of Danio rerio. Sci. Total Environ. 799, 149432.
Kalkavan, H., Green, D.R., 2018. MOMP, cell suicide as a BCL-2 family business. Cell Death & Differentiation 25 (1), 46–55.
Kastenhuber, E.R., Lowe, S.W., 2017. Putting p53 in context. Cell 170 (6), 1062–1078.
Kim, J.H., Park, K.S., Hong, A.R., Shin, C.S., Kim, S.Y., Kim, S.W., 2016. Diagnostic role of captopril challenge test in Korean subjects with high aldosterone-to-renin ratios. Endocrinol. Metab. 31 (2), 277–283.
Kimmel, C.B., Ballard, W.W., Kimmel, S.R., Ullmann, B., Schilling, T.F., 1995. Stages of embryonic development of the zebrafish. Dev. Dyn. 203, 253–310. https://doi.org/10.1002/aja.1002030302.
Kondratskyi, A., Kondratska, K., Skryma, R., Prevarskaya, N., 2015. Ion channels in the regulation of apoptosis. Biochimica et Biophysica Acta (BBA)-Biomembranes 1848 (10), 2532–2546.
Kovesdy, C.P., 2014. Management of hyperkalaemia in chronic kidney disease. Nat. Rev. Nephrol. 10 (11), 653–662.
Mahmoud, W.M., Kümmerer, K., 2012. Captopril and its dimer captopril disulfide: Photodegradation, aerobic biodegradation and identification of transformation products by HPLC–UV and LC–ion trap-MSn. Chemosphere 88 (10), 1170–1177.
Mc Namara, K., Alzubaidi, H., Jackson, J.K., 2019. Cardiovascular disease as a leading cause of death: how are pharmacists getting involved? Integrated pharmacy research and practice 1–11.
Nalecz-Jawecki, G., Persoone, G., 2006. Toxicity of selected pharmaceuticals to the anostracan crustacean Thamnocephalus platyurus-comparison of sublethal and lethal effect levels with the 1h Rapidtoxkit and the 24h Thamnotoxkit microbiotests. Environ. Sci. Pollut. Res. 13, 22–27.
Naylor, R.W., Qubisi, S.S., Davidson, A.J., 2017. Zebrafish pronephros development. Kidney development and disease 27–53.
Nguyen, T.K., Petrikas, M., Chambers, B.E., Wingert, R.A., 2023. Principles of zebrafish nephron segment development. Journal of Developmental Biology 11 (1), 14.
Parekh, A., 2024a. UK Cardiovascular Drugs Market Analysis Report 2022 to 2030, Insights10. https://www.insights10.com/report/uk-cardiovascular-drugs-market-analysis/.
Parekh, A., 2024b. Canada Cardiovascular Drugs Market Analysis Report 2022 to 2030, Insights10. https://www.insights10.com/report/canada-cardiovascular-drugs-market-analysis/.
Pfaffl, M.W., 2001. A new mathematical model for relative quantification in real-time RT–PCR. Nucleic Acids Res. 29 (9), e45.
Pfaffl, M.W., Horgan, G.W., Dempfle, L., 2002. Relative expression software tool (REST©) for group-wise comparison and statistical analysis of relative expression results in real-time PCR. Nucleic Acids Res. 30 (9), e36.
Prowle, J.R., Echeverri, J.E., Ligabo, E.V., Ronco, C., Bellomo, R., 2010. Fluid balance and acute kidney injury. Nat. Rev. Nephrol. 6 (2), 107–115.
Ramírez, A., Vázquez-Sánchez, A.Y., Carrión-Robalino, N., Camacho, J., 2016. Ion channels and oxidative stress as a potential link for the diagnosis or treatment of liver diseases. Oxid. Med. Cell. Longev. 2016.
Saha, T., Gautam, A., Mukherjee, A., Lahiri, M., Talukdar, P., 2016. Chloride transport through supramolecular barrel-rosette ion channels: lipophilic control and apoptosis-inducing activity. J. Am. Chem. Soc. 138 (50), 16443–16451.
Schmittgen, T.D., Livak, K.J., 2008. Analyzing real-time PCR data by the comparative CT method. Nat. Protoc. 3, 1101–1108. https://doi.org/10.1038/nprot.2008.73.
Scott, J.H., Menouar, M.A., Dunn, R.J., 2017. Physiology, Aldosterone.
Sedletcaia, A., Evans, T., 2011. Heart chamber size in zebrafish is regulated redundantly by duplicated tbx2 genes. Dev. Dyn. 240 (6), 1548–1557.
Soi, V., Yee, J., 2017. Sodium homeostasis in chronic kidney disease. Adv. Chronic Kidney Dis. 24 (5), 325–331.
Thi Thu, H.N., Haw Tien, S.F., Loh, S.L., Bok Yan, J.S., Korzh, V., 2013. tbx2a is required for specification of endodermal pouches during development of the pharyngeal arches. PloS One 8 (10), e77171.
Westhoff, J.H., Giselbrecht, S., Schmidts, M., Schindler, S., Beales, P.L., Tönshoff, B., Gehrig, J., 2013. Development of an automated imaging pipeline for the analysis of the zebrafish larval kidney. PloS One 8 (12), e82137.
Wingert, R.A., Davidson, A.J., 2011. Zebrafish nephrogenesis involves dynamic spatiotemporal expression changes in renal progenitors and essential signals from retinoic acid and irx3b. Dev. Dyn. 240 (8), 2011–2027.
Yang, H., Xie, Y., Yang, D., Ren, D., 2017. Oxidative stress-induced apoptosis in granulosa cells involves JNK, p53 and Puma. Oncotarget 8 (15), 25310.
Zhang, M., Zheng, J., Nussinov, R., Ma, B., 2017. Release of cytochrome C from Bax pores at the mitochondrial membrane. Sci. Rep. 7 (1), 2635.